Dynamics of Droplet Pinch-Off at Emulsified Oil-Water Interfaces: Interplay between Interfacial Viscoelasticity and Capillary Forces

Parisa Bazazi,[1,*] Howard A. Stone,[2] and S. Hossein Hejazi[1,†]

[1]*Department of Chemical and Petroleum Engineering, University of Calgary, Calgary, Alberta T2N 1N, Canada*

[2]*Department of Mechanical and Aerospace Engineering, Princeton University, Princeton, New Jersey 08544, USA*

(Received 5 June 2022; revised 16 October 2022; accepted 20 December 2022; published 18 January 2023)

The presence of submicrometer structures at liquid-fluid interfaces modifies the properties of many science and technological systems by lowering the interfacial tension, creating tangential Marangoni stresses, and/or inducing surface viscoelasticity. Here we experimentally study the break-up of a liquid filament of a silica nanoparticle dispersion in a background oil phase that contains surfactant assemblies. Although self-similar power-law pinch-off is well documented for threads of Newtonian fluids, we report that when a viscoelastic layer is formed *in situ* at the interface, the pinch-off dynamics follows an exponential decay. Recently, such exponential neck thinning was found theoretically when surface viscous effects were taken into account. We introduce a simple approach to calculate the effective relaxation time of viscoelastic interfaces and estimate the thickness of the interfacial layer and the viscoelastic properties of liquid-fluid interfaces, where the direct measurement of interfacial rheology is not possible.

DOI: 10.1103/PhysRevLett.130.034001

Introduction.—In many situations, including the dripping of liquid from a leaky faucet and the formation of droplets in an inkjet printer [1–5], a transient liquid filament connects a droplet to the rest of the fluid. Unconfined liquid threads are unstable and eventually form droplets to minimize the surface energy with the surrounding fluid [6,7]. The dynamics of such droplet pinch-off has been studied extensively for various systems, from pure Newtonian fluids [8,9] to complex non-Newtonian liquids [10–14]. In many cases the thinning dynamics for Newtonian liquids is self-similar and evolves through various regimes that are characterized by the reduction of the minimum neck radius (h_{min}) with the time to pinch-off ($\tau = t_p - t$) as $h_{min} \sim \tau^{\alpha}$, where t_p is the time instant that pinch-off occurs and t is the time of the experiment [7–9,15–19].

Surfactants are widely used in inkjet printing and spray drying applications to keep droplets stable after their formation [20,21]. The self-similar breakup dynamics characteristic of clean jets is evident also when surfactants are present [22]. The addition of surfactants reduces the surface tension and consequently the capillary pressure, which is the driving force for pinch-off; thus, the breakup of a surfactant-laden thread is slower than that of pure liquid [23–27]. For surfactant concentrations below the critical micelle concentration, as fluid is expelled from the thread's neck, surfactants are swept away from the neck region, which produces Marangoni stresses that tend to further slow thinning [24,25,28,29]. In addition, the assembly of surfactants at the interface, on account of their size and structure, can lead to a more complex surface rheology, which may show liquidlike (viscous) or solidlike (elastic) behavior at the interface. So, aside from the effect of surfactants on the interfacial tension reduction and Marangoni stress generation, the surface rheological effects, due to the surfactant network at the interface, may affect the dynamics of the pinch-off [30–34].

The influence of interfacial shear and dilatation viscosity on droplet pinch-off, other than one pioneering study in 1980 [30], has not been the focus of research until recently [31–33,35]. For example, Ponce-Torres and co-workers theoretically and experimentally examined the pinch-off dynamics of water droplets in air in the presence of insoluble [31] and soluble surfactants [32] and found that when Marangoni and surface viscous stresses are important, surfactants are not swept away from the thread neck. Interfacial viscosity resists the driving capillary pressure close to the breakup, where pinch-off occurs in the viscocapillary regime [32]. In particular, in recent theoretical studies on Newtonian viscous interfacial layers, it was shown that when the thread interface is fully saturated with surfactants the thinning dynamics is governed by a balance of surface viscosity and surface tension, and the neck radius decays exponentially with time [33,35], while a linear decay has been reported if the surfactant concentration changes over time [33]. However, this exponential regime has not been confirmed through experiments.

For practical physical systems, we can expect that interfaces are not purely viscous and they may also have elastic properties. Despite the rich literature on the pinch-off of non-Newtonian fluids [10–14], the effect of interfacial viscoelasticity on the dynamics of thread breakup has not been studied. In this Letter, we experimentally investigate the droplet pinch-off dynamics in immiscible

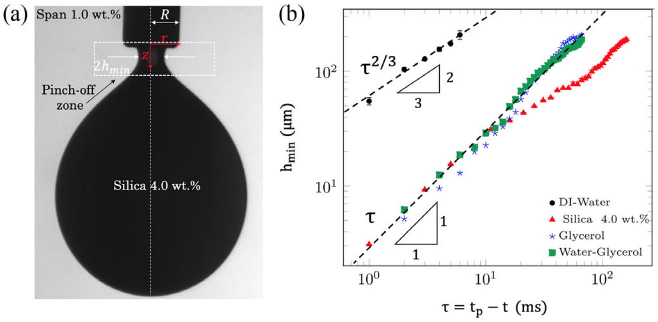

FIG. 1. The dynamics of droplet pinch-off. (a) Schematic of droplet pinch-off. (b) Minimum neck radius versus time to pinch-off for DI water (black), 4.0 wt.% silica dispersion (red), glycerol (blue), and a water-glycerol mixture (5%, v/v) (green) in Span 1.0 wt.% micellar solution. Representative error bars are shown.

liquid-liquid systems, when viscoelastic materials are generated *in situ* at the interface and discuss how non-Newtonian interfaces change the neck thinning dynamics of Newtonian liquids.

Results.—The aqueous phase is injected vertically with a fixed flow rate of 0.1 μl/s (injection speed of $\sim 8 \times 10^{-4}$ m/s) using a needle with inner diameter (D) of 0.4 mm into a glass cuvette filled with 1.0 wt.% Sorbitane monooleate (Span 80) micellar solutions (see Supplemental Material [36]), as shown in Fig. 1(a). After the injection, the droplet is approximately at rest for 10 sec before the thinning starts. We record the thinning of the liquid thread with a camera (Kruss, DSA 100) at 1000 frames per sec (fps) and a resolution of 6.1 μm/pixel, resulting in the time history of the minimum thread radius $h_{\rm min}(\tau)$.

We first present the thinning dynamics of a water thread with the equilibrium interfacial tension of $\gamma_{\rm eq} \sim 2.5$ mN/m and Ohnesorge number, $Oh = \mu/\sqrt{\rho\gamma_{\rm eq} R} = 0.04$, where μ, ρ, and R are, respectively, the viscosity, density, and radius of the thread, Fig. 1(b). For water (black circles), the neck radius decreases with $\tau^{2/3}$, which is known as the capillary-inertia regime, i.e., $h_{\rm min} = A(\gamma_{\rm eq}/\rho)^{1/3}\tau^{2/3}$, where A is the prefactor [9,18,37–39]. The magnitude of the prefactor can be estimated from the slope of the line, which yields $A = 0.47$; theory predicts $A \approx 0.717$ while experiments show $0.4 \lesssim A \lesssim 0.6$ [37]. The constant slope of $h_{\rm min}$ versus τ in a log-log plot in Fig. 1(b), i.e., the prefactor A for DI water, also suggests the absence of Marangoni stresses at the surfactant concentration of 1.0 wt.% (880 times the CMC) used in these experiments [27]. The length scale of the minimum neck radius prior to breakup, estimated from $\mu^2/(\gamma_{\rm eq}\rho)$ [7], is less than a micrometer, which precludes capturing the dynamics close to pinch-off.

The minimum neck radius of a 4.0 wt.% silica dispersion drop with $\gamma_{\rm eq} \sim 0.2$ mN/m and Oh = 0.16 (red triangles) as a function of τ, when reported on a log-log plot, exhibits a linear flow regime prior to pinch-off and a nonlinear regime at early times. The neck thinning of the silica dispersion is neither dominated by inertia as expected for low viscosity fluids [9] nor by diffusion ($\tau^{1/3}$) as expected for low interfacial tension fluids (near-miscible aqueous two phase systems) [40]. However, the linear pinch-off dynamics has been previously reported for high viscosity fluids with Oh $\gtrsim 1$. Thus, we examine the similarities in pinch-off dynamics of silica dispersion droplets and a high viscosity fluid, i.e., a glycerol drop (Oh = 52) and a glycerol-water (5%, v/v) mixture (Oh = 22), with $\gamma_{\rm eq} \sim 2.5$ mN/m (see Supplemental Material [36]). Unlike the aforementioned multiple regimes in the silica dispersion case, the minimum neck radii of the glycerol droplet (blue stars) and the glycerol-water (green square) in Fig. 1(b) linearly decreases over time throughout the entire process (see Supplemental Material [36,41]).

The images in Figs. 2(a)–2(c) show that for water, glycerol, and glycerol-water, pinch-off occurs simultaneously at two locations, which straddle a satellite droplet. The water thread connects two drops, nearly conical in shape, where the minimum radius is near the thread's center for about 5 ms before the occurrence of the two minima close to the separating droplets. During the pinch-off in both the low

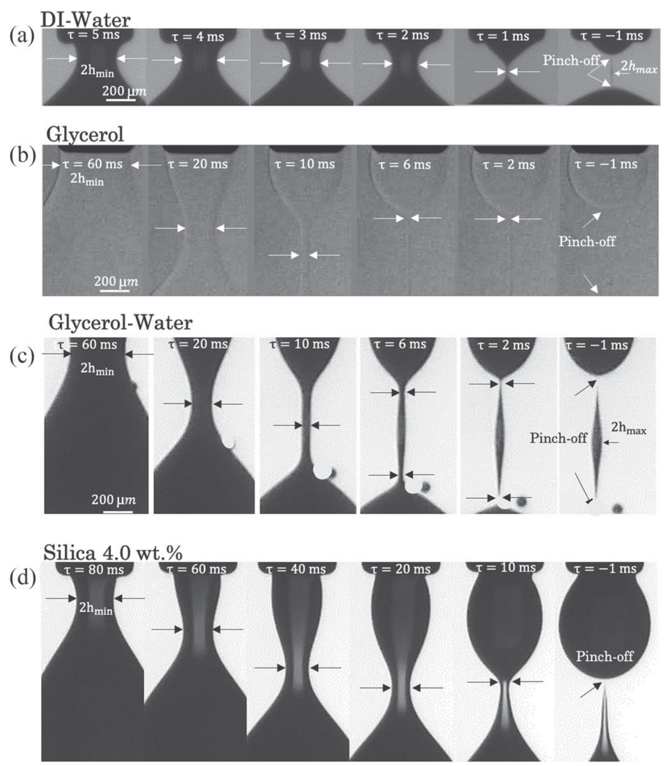

FIG. 2. Images of droplet pinch-off that highlight the role of interfacial viscoelasticity on the neck thinning dynamics. (a) DI water, (b) glycerol mixture, (c) 4.0 wt.% silica dispersion, and (d) glycerol-water (5%, v/v). Although the silica dispersion droplet has a viscosity close to that of DI-water, its pinch-off occurs at a single point, which is not similar to the pinch-off of liquids with Oh < 1 or liquids with Oh > 1.

viscosity [Fig. 2(a)] and high viscosity [Figs. 2(b)–2(c)] cases, the fluid is expelled from the center of the filament toward the ends, as, by symmetry, there is a mid-plane stagnation point, which experiences pressure buildup. Consequently, the minimum neck radius moves away from the midplane towards the filament ends, forming two minima close to the separating droplets. This pinch-off is self-similar and has been reported for a variety of Newtonian fluids through experiments and simulations [16,42,43].

In contrast, the shape of the neck in the silica dispersion drop is asymmetric, where the pinch-off occurs at the rear of the filament [the last two panels in Fig. 2(d)]. The thread is initially close to cylindrical in shape, and then transitions into an asymmetric neck connecting a more rounded droplet to a nearly conical shape at the later stages. The minimum neck radius is located near the top end of the thread. No satellite droplet is formed for the silica case. This type of pinch-off, known as exit pinch-off, has been reported previously for non-Newtonian polymer solutions, and is governed by a balance of elastic and capillary forces [14,44]. The similarity in the pinch-off location and the thread shape between the silica dispersion and bulk non-Newtonian fluids signals the possible generation of an interfacial viscoelastic skin, as shown next, which can affect the pinch-off dynamics.

A concentrated silica dispersion (4.0 wt.% concentration), upon contact with Span 80 micellar solution (10.0 wt.% concentration), can spontaneously form structured layers of emulsions embedded in the oil, with a thickness on the order of one micrometer, in the vicinity of the fluid-fluid interface [45,46]. The possibility of forming such an interfacial material for the present system, which is at a lower Span concentration, is investigated by forming a pendant drop of silica dispersion in the micellar solution. In particular, Fig. 3(a) shows a pendant drop connected to a syringe to apply a compression and expansion cycle. The liquid is withdrawn from the silica dispersion droplet during the first 100 sec where wrinkles are observed at the interface within the first 6–7 sec (see Supplemental Material [36] and movie S1). Upon re-injection of liquid, the interface returns to its original state. The wrinkle formation and disappearance by compression and expansion cycles indicate the presence of a viscoelastic skin at the droplet's interface, which is the emulsion phase [as shown in the inset of Fig. 3(b)] with distinct rheological characteristics.

We carried out shear and frequency sweep tests on the *in situ* generated emulsion phase (see Supplemental Material [36,47,48]) and the results confirm the viscoelastic properties of the emulsion layer [Figs. 3(b)–3(c)]. The rheology of the material at a dynamic interface is more complex, so we first compute numerically the range of shear or extension rates occurring during the neck thinning process of a silica dispersion at the pinch-off location as

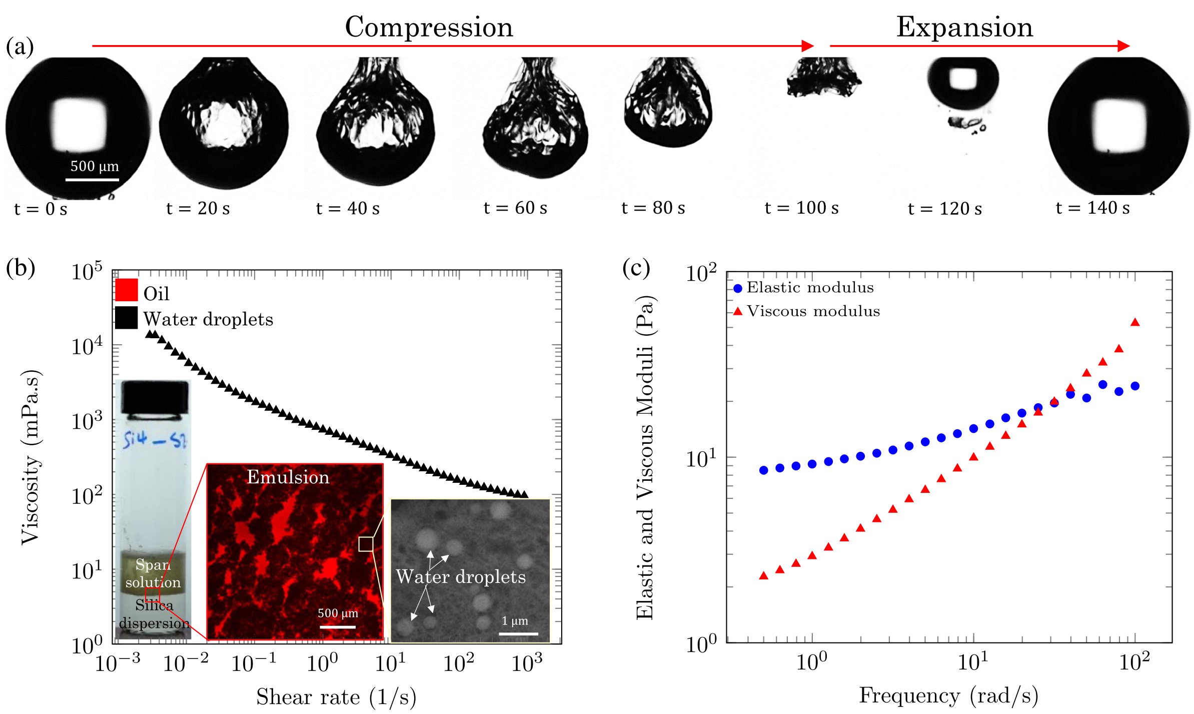

FIG. 3. Rheological properties of the interfacial layer. (a) Formation of an interfacial layer at the silica dispersion droplet-Span micellar solution interface. (b) Shear viscosity of the emulsion phase at the oil-water interface. The inset shows a confocal image of the collected emulsion phase from the silica dispersion-micellar solution interface. The red color shows the oil phase and the black zone represents the submicrometer water droplets. (c) Frequency sweep test of the emulsion.

$(dh_{\min}/d\tau)/D$. As shown in Fig. S3, the average shear or extension rate at the pinch-off location is $\sim 3\ s^{-1}$. The emulsion phase at this shear rate has the viscosity of $\approx$520 mPa.s [Fig. 3(b)]. We do not have an approach to directly measure the extensional viscosity and recognize that the shear viscosity is different from the extensional viscosity as the liquid filament experiences an extension during the pinch-off. However, shear and extensional viscosities should have a comparable order of magnitude as long as long-chain polymer molecules are not involved [49].

The formation of the emulsion phase at the silica dispersion-Span micellar solution interface creates a viscoelastic skin that affects the dynamics of the droplet pinch-off. Since the thinning of bulk viscoelastic threads undergoes an exponential decay [10–14], we examine the possibility of such an exponential thinning dynamics for the silica dispersion drop. The measurement of the thinning for a silica dispersion drop is reported on a semi-log plot of the minimum neck radius versus time and exhibits an initial exponential decay, $h_{\min} \propto e^{-\omega t}$, for about 100 ms with $\omega \sim 12\ s^{-1}$, which then transitions into a linear regime prior to pinch-off [blue triangles, Fig. 4(a)]. The effective relaxation time constant, λ_e, is the time constant of the exponential regime ($h_{\min} \sim e^{-t/3\lambda_e}$) [14], which is about 28 ms, shown in Fig. 4(a). Since λ_e is shorter than the shortest relaxation time [calculated from the crossover of viscous and elastic moduli in Fig. 3(c) to be $\lambda \approx 32$ ms], the reported exponential decay for the silica dispersion droplet with a viscoelastic interface differs from the bulk viscoelastic materials [14].

To differentiate between the pinch-off dynamics of viscoelastic interfaces and viscoelastic bulk materials, we analyzed the thinning dynamics of the emulsion sample collected from the interface of a silica dispersion-Span micellar solution, which was previously used for the viscosity and rheology experiments. The emulsion drop is formed with the injection flow rate of 0.1 μl/s in Span micellar solution and neck thinning is recorded over time [Fig. 4(b)]. The thinning of the emulsion drop also shows an exponential decay [black stars, Fig. 4(a)], however, unlike systems where interfacial viscoelastic materials are formed *in situ* at the oil-water interface, the effective relaxation time (47 ms) is longer than the shortest relaxation time of the emulsion sample, confirming that the pinch-off is dominated by the elastocapillary regime for the bulk emulsion system. The emulsion drop exhibits a linear decay before the breakup, which could be an indication of alignment of emulsion droplets under strong extensional flow, where the pinch-off occurs in the finite extensibility regime (Supplemental Material [36,49–52]).

The exponential thread thinning regime has been reported for viscous interfacial layers in theoretical work [33,35]. In our experiments, the local Boussinesq number is greater than 1, hence, the surface viscous effects are expected to be more significant than the bulk viscous effects (see Supplemental Material [35,36]). The elastic forces can overcome the capillary forces at length scales below 0.1 μm, which is much smaller than the minimum neck radius in the exponential thinning regime of our experiments (see Supplemental Material [36,53–57]). Therefore, the reported exponential decay for the silica dispersion droplet can result from the balance of surface viscous stresses with the capillary forces [35]. The linear regime prior to the pinch-off [Fig. 4(a)] could be due to the nonuniform distribution of emulsions at the interface when the rate of the interface expansion is fast and interface is not fully covered with the viscoelastic skin, similar to the viscous interfaces with surfactants [33].

In the presence of surface viscous stresses, the pinch-off follows $h_{\min} \sim e^{-F(\Theta)t/t_c}$, where $t_c = (3\mu_s + k_s)/\gamma$ is the characteristic timescale, μ_s is the surface shear viscosity, k_s is the surface dilatational viscosity, and $\Theta = k_s/\mu_s$. $F(\Theta)$ is a universal function that varies between 0.113 to 0.225

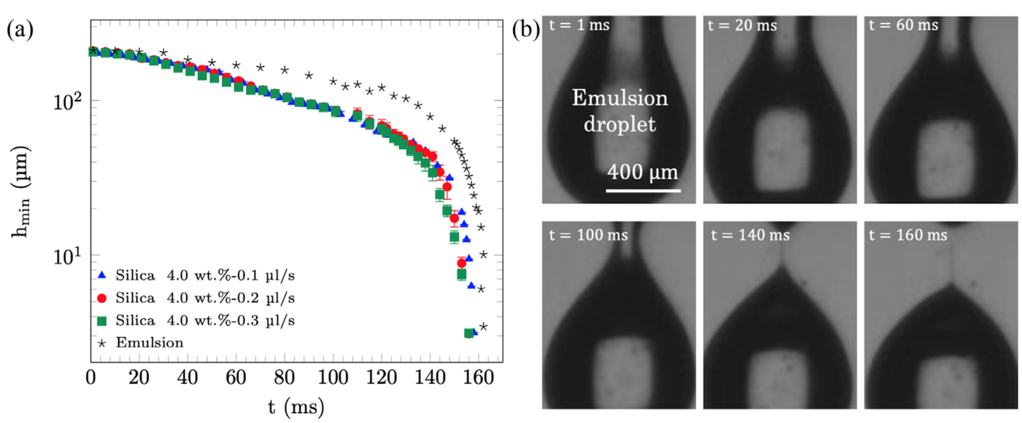

FIG. 4. Effect of viscoelasticity on the pinch-off. (a) Minimum neck radius over time for the silica dispersion droplet that is formed with the injection flow rates of 0.1, 0.2, and 0.3 μl/s in blue, red, and green, respectively. The neck thinning of a bulk phase emulsion droplet formed with 0.1 μl/s flow rate is shown in black. (b) Images of the emulsion droplet during the neck thinning.

when Θ changes from 0.1 to 10 [35,58]. For a thin layer of a Newtonian fluid with the viscosity μ on top of a second fluid, the shear and dilatational surface viscosities can be estimated as $\mu_s = \mu b$ and $k_s = 3\ \mu b$, respectively, where b is the film thickness [59]. Considering $F(\Theta = 3) = 0.166$ [35], substituting the surface shear and dilatation viscosity equations into the exponential decay ($h_{\min} \sim e^{-F(\Theta)t/t_c}$), and equating it with the time constant of the exponential decay plot ($h_{\min} \sim e^{-\omega t}$), the thickness of the interfacial layer is obtained as 0.9 μm, which is within the range of the diameters of the emulsion droplets (100 nm − 1 μm) [45,46]. The interfacial material may consist of single or several emulsion droplets, so the magnitude of the calculated thickness is plausible, although the interface might be thicker. Thus, the estimated thickness from the exponential decay time constant also confirms the formation of an interfacial layer at the silica dispersion-Span micellar solution interface.

We further extend this analysis to two other silica-Span systems (silica 10.0 wt.%-Span 1.0 wt.% and silica 10.0 wt.%-Span 2.0 wt.%), Fig. S5, for which we expect an enhanced emulsification rate and consequently an increased interfacial layer thickness. Increasing the concentration of particles from 4.0 to 10.0 wt.% and surfactants from 1.0 to 2.0 wt.% slightly increases the computed thickness of the interfacial layer to 1.3 and 2.5 μm, respectively. The *in situ* generated viscoelastic interfacial layer in this Letter follows the exponential decay of viscous interfaces and the thickness of emulsion layers can be estimated based on the properties of the materials and the dynamics of the droplet pinch-off.

The effect of resting time on the pinch-off dynamics is distinguished by conducting two experiments where the silica droplets are formed with the injection flow rates of 0.2 and 0.3 μl/s [Fig. 4(a)]. In these cases, resting time before pinch-off is 3–5 sec, the neck thinning follows the same trend as the droplet formed with the injection flow rate of 0.1 μl/s (10 sec resting time); see Supplemental Material [36]. Although the thickness of the emulsion layer may increase over time, the resting time does not significantly affect the pinch-off dynamics (Fig. S4 [36]).

Conclusion.—We studied the role of interfacial materials on the droplet pinch-off dynamics. Two such regimes are distinguished when silica nanoparticles are added to the system: (i) an exponential neck thinning regime with $\mathrm{h}_{\min} \sim \mathrm{e}^{-\omega t}$, and (ii) a linear regime with $\mathrm{h}_{\min} \sim \tau$ prior to the neck rupture. The surface viscoelasticity, triggered by the *in situ* generation of emulsion at the thread interface during the experimental timescale, is responsible for the change in the pinch-off dynamics of Newtonian fluid threads. The interface elasticity allows the droplet to wrinkle and interface viscosity resists the pinch-off. Controlling the pinch-off process in the presence of *in situ* generated interfacial materials is a critical step in many 3D printing process including dropwise additive manufacturing and direct ink writing techniques. Our experimental findings and interpretation offer a guideline for the future numerical and theoretical research on the influence of interfacial viscoelasticity on the drop pinch-off dynamics.

This study was financially funded by Natural Sciences and Engineering Research Council of Canada (NSERC) Discovery Grant No. RGPIN/07186-2019, University of Calgary's Canada First Research Excellence Fund (CFREF) program, and the Global Research Initiative (GRI) in Sustainable Low Carbon Unconventional Resources. We also gratefully acknowledge infrastructure funding from Canadian Foundation for Innovation (CFI) CFI JELF 33700. P. B. appreciates Alberta Innovates and the University of Calgary Eyes High Graduate Student Scholarships.

[*]Corresponding author.
parisa.bazazi@princeton.edu
[†]Corresponding author.
shhejazi@ucalgary.ca

[1] G. Villar, A. D. Graham, and H. Bayley, A tissue-like printed material, Science **340**, 48 (2013).

[2] H. J. Mea, L. Delgadillo, and J. Wan, On-demand modulation of 3d-printed elastomers using programmable droplet inclusions, Proc. Natl. Acad. Sci. U.S.A. **117**, 14790 (2020).

[3] D. Lohse, Fundamental fluid dynamics challenges in inkjet printing, Annu. Rev. Fluid Mech. **54**, 349 (2022).

[4] C. B. Highley, K. H. Song, A. C. Daly, and J. A. Burdick, Jammed microgel inks for 3d printing applications, Adv. Sci. **6**, 1801076 (2019).

[5] A. Toor, B. A. Helms, and T. P. Russell, Effect of nanoparticle surfactants on the breakup of free-falling water jets during continuous processing of reconfigurable structured liquid droplets, Nano Lett. **17**, 3119 (2017).

[6] L. Rayleigh, On the instability of jets, Proc. London Math. Soc. **s1-10**, 4 (1878).

[7] J. Eggers and E. Villermaux, Physics of liquid jets, Rep. Prog. Phys. **71**, 036601 (2008).

[8] J. R. Lister and H. A. Stone, Capillary breakup of a viscous thread surrounded by another viscous fluid, Phys. Fluids **10**, 2758 (1998).

[9] J. R. Castrejón-Pita, A. A. Castrejón-Pita, S. S. Thete, K. Sambath, I. M. Hutchings, J. Hinch, J. R. Lister, and O. A. Basaran, Plethora of transitions during breakup of liquid filaments, Proc. Natl. Acad. Sci. U.S.A. **112**, 4582 (2015).

[10] S. L. Anna and G. H. McKinley, Elasto-capillary thinning and breakup of model elastic liquids, J. Rheol. **45**, 115 (2001).

[11] Y. Amarouchene, D. Bonn, J. Meunier, and H. Kellay, Inhibition of the Finite-Time Singularity During Droplet Fission of a Polymeric Fluid, Phys. Rev. Lett. **86**, 3558 (2001).

[12] C. Wagner, Y. Amarouchene, D. Bonn, and J. Eggers, Droplet Detachment and Satellite Bead Formation in Viscoelastic Fluids, Phys. Rev. Lett. **95**, 164504 (2005).

[13] R. Sattler, S. Gier, J. Eggers, and C. Wagner, The final stages of capillary break-up of polymer solutions, Phys. Fluids **24**, 023101 (2012).

[14] C. Xu, Z. Zhang, J. Fu, and Y. Huang, Study of pinch-off locations during drop-on-demand inkjet printing of viscoelastic alginate solutions, Langmuir **33**, 5037 (2017).

[15] J. B. Keller and M. J. Miksis, Surface tension driven flows, SIAM J. Appl. Math. **43**, 268 (1983).

[16] Y.-J. Chen and P. H. Steen, Dynamics of inviscid capillary breakup: Collapse and pinchoff of a film bridge, J. Fluid Mech. **341**, 245 (1997).

[17] R. F. Day, E. J. Hinch, and J. R. Lister, Self-Similar Capillary Pinchoff of an Inviscid Fluid, Phys. Rev. Lett. **80**, 704 (1998).

[18] J. Eggers, Nonlinear dynamics and breakup of free-surface flows, Rev. Mod. Phys. **69**, 865 (1997).

[19] D. Leppinen and J. R. Lister, Capillary pinch-off in inviscid fluids, Phys. Fluids **15**, 568 (2003).

[20] E. Antonopoulou, O. G. Harlen, M. Rump, T. Segers, and M. A. Walkley, Effect of surfactants on jet break-up in drop-on-demand inkjet printing, Phys. Fluids **33**, 072112 (2021).

[21] P. Dastyar, M. S. Salehi, B. Firoozabadi, and H. Afshin, Influences of polymer–surfactant interaction on the drop formation process: An experimental study, Langmuir **37**, 1025 (2021).

[22] R. V. Craster, O. K. Matar, and D. T. Papageorgiou, Pinchoff and satellite formation in surfactant covered viscous threads, Phys. Fluids **14**, 1364 (2002).

[23] V. G. Levich and V. S. Krylov, Surface-tension-driven phenomena, Annu. Rev. Fluid Mech. **1**, 293 (1969).

[24] H. A. Stone and L. G. Leal, The effects of surfactants on drop deformation and breakup, J. Fluid Mech. **220**, 161 (1990).

[25] W. J. Milliken, H. A. Stone, and L. G. Leal, The effect of surfactant on the transient motion of newtonian drops, Phys. Fluids A **5**, 69 (1993).

[26] M. Roché, M. Aytouna, D. Bonn, and H. Kellay, Effect of Surface Tension Variations on the Pinch-Off Behavior of Small Fluid Drops in the Presence of Surfactants, Phys. Rev. Lett. **103**, 264501 (2009).

[27] N. M. Kovalchuk, E. Nowak, and M. J. H. Simmons, Effect of soluble surfactants on the kinetics of thinning of liquid bridges during drops formation and on size of satellite droplets, Langmuir **32**, 5069 (2016).

[28] P. T. McGough and O. A. Basaran, Repeated Formation of Fluid Threads in Breakup of a Surfactant-Covered Jet, Phys. Rev. Lett. **96**, 054502 (2006).

[29] P. M. Kamat, B. W. Wagoner, S. S. Thete, and O. A. Basaran, Role of marangoni stress during breakup of surfactant-covered liquid threads: Reduced rates of thinning and microthread cascades, Phys. Rev. Fluids **3**, 043602 (2018).

[30] A. Hajiloo, T. R. Ramamohan, and J. C. Slattery, Effect of interfacial viscosities on the stability of a liquid thread, J. Colloid Interface Sci. **117**, 384 (1987).

[31] A. Ponce-Torres, J. M. Montanero, M. A. Herrada, E. J. Vega, and J. M. Vega, Influence of the Surface Viscosity on the Breakup of a Surfactant-Laden Drop, Phys. Rev. Lett. **118**, 024501 (2017).

[32] A. Ponce-Torres, M. Rubio, M. A. Herrada, J. Eggers, and J. M. Montanero, Influence of the surface viscous stress on the pinch-off of free surfaces loaded with nearly-inviscid surfactants, Sci. Rep. **10**, 16065 (2020).

[33] H. Wee, B. W. Wagoner, P. M. Kamat, and O. A. Basaran, Effects of Surface Viscosity on Breakup of Viscous Threads, Phys. Rev. Lett. **124**, 204501 (2020).

[34] H. Wee, B. W. Wagoner, V. Garg, P. M. Kamat, and O. A. Basaran, Pinch-off of a surfactant-covered jet, J. Fluid Mech. **908**, A38 (2021).10.1017/jfm.2020.801

[35] A. Martínez-Calvo and A. Sevilla, Universal Thinning of Liquid Filaments under Dominant Surface Forces, Phys. Rev. Lett. **125**, 114502 (2020).

[36] See Supplemental Material at http://link.aps.org/supplemental/10.1103/PhysRevLett.130.034001 for the details of experimental protocols, interfacial tension, and rheology data.

[37] A. Deblais, M. A. Herrada, I. Hauner, K. P. Velikov, T. Van Roon, H. Kellay, J. Eggers, and D. Bonn, Viscous Effects on Inertial Drop Formation, Phys. Rev. Lett. **121**, 254501 (2018).

[38] D. H. Peregrine, G. Shoker, and A. Symon, The bifurcation of liquid bridges, J. Fluid Mech. **212**, 25 (1990).

[39] X. Jiang, E. Xu, X. Meng, and H. Z. Li, The effect of viscosity ratio on drop pinch-off dynamics in two-fluid flow, J. Ind. Eng. Chem. **91**, 347 (2020).

[40] H. Y. Lo, Y. Liu, S. Y. Mak, Z. Xu, Y. Chao, K. J. Li, H. C. Shum, and L. Xu, Diffusion-Dominated Pinch-Off of Ultralow Surface Tension Fluids, Phys. Rev. Lett. **123**, 134501 (2019).

[41] D. T. Papageorgiou, Analytical description of the breakup of liquid jets, J. Fluid Mech. **301**, 109 (1995).

[42] N. M. Kovalchuk, E. Nowak, and M. J. H. Simmons, Kinetics of liquid bridges and formation of satellite droplets: Difference between micellar and bi-layer forming solutions, Colloids Surf. A **521**, 193 (2017).

[43] P. Doshi, I. Cohen, W. W. Zhang, M. Siegel, P. Howell, O. A. Basaran, and S. R. Nagel, Persistence of memory in drop breakup: The breakdown of universality, Science **302**, 1185 (2003).

[44] A. M. Ardekani, V. Sharma, and G. H. McKinley, Dynamics of bead formation, filament thinning and breakup in weakly viscoelastic jets, J. Fluid Mech. **665**, 46 (2010).

[45] P. Bazazi and S. H. Hejazi, Spontaneous formation of double emulsions at particle-laden interfaces, J. Colloid Interface Sci. **587**, 510 (2021).

[46] P. Bazazi, H. A. Stone, and S. H. Hejazi, Spongy all-in-liquid materials by in-situ formation of emulsions at oil-water interfaces, Nat. Commun. **13**, 4162 (2022).

[47] N. Alexandrov, K. G. Marinova, K. D. Danov, and I. B. Ivanov, Surface dilatational rheology measurements for oil/water systems with viscous oils, J. Colloid Interface Sci. **339**, 545 (2009).

[48] D. Renggli, A. Alicke, R. H. Ewoldt, and J. Vermant, Operating windows for oscillatory interfacial shear rheology, J. Rheol. **64**, 141 (2020).

[49] S. Różańska, J. Różański, M. Ochowiak, and P. Mitkowski, Extensional viscosity measurements of concentrated emulsions with the use of the opposed nozzles device, Braz. J. Chem. Eng. **31**, 47 (2014).

[50] M. Renardy, Similarity solutions for jet breakup for various models of viscoelastic fluids, J. Nonnewton. Fluid. Mech. **104**, 65 (2002).

[51] S. Różańska, L. Broniarz-Press, J. Różański, P. Mitkowski, M. Ochowiak, and S. Woziwodzki, Extensional viscosity and stability of oil-in-water emulsions with addition poly (ethylene oxide), Procedia Eng. **42**, 733 (2012).

[52] G. G. Warr, Shear and elongational rheology of ternary microemulsions, Colloids Surf. A **103**, 273 (1995).

[53] H. Manikantan and T. M. Squires, Pressure-dependent surface viscosity and its surprising consequences in interfacial lubrication flows, Phys. Rev. Fluids **2**, 023301 (2017).

[54] R. Dimova, U. Seifert, B. Pouligny, S. Förster, and H.-G. Döbereiner, Hyperviscous diblock copolymer vesicles, Eur. Phys. J. E **7**, 241 (2002).

[55] R. Dimova, S. Aranda, N. Bezlyepkina, V. Nikolov, K. A. Riske, and R. Lipowsky, A practical guide to giant vesicles. probing the membrane nanoregime via optical microscopy, J. Phys. Condens. Matter **18**, S1151 (2006).

[56] O.-Y. Zhong-Can and W. Helfrich, Instability and Deformation of a Spherical Vesicle by Pressure, Phys. Rev. Lett. **59**, 2486 (1987).

[57] R. Lipowsky, Coupling of bending and stretching deformations in vesicle membranes, Adv. Colloid Interface Sci. **208**, 14 (2014).

[58] A. Martínez-Calvo and A. Sevilla, Temporal stability of free liquid threads with surface viscoelasticity, J. Fluid Mech. **846**, 877 (2018).

[59] A. D. Jenkins and K. B. Dysthe, The effective film viscosity coefficients of a thin floating fluid layer, J. Fluid Mech. **344**, 335 (1997).